Eur. Phys. J. A **20**, 9–14 (2004)
DOI 10.1140/epja/i2002-10312-5

THE EUROPEAN PHYSICAL JOURNAL A

Gamma-ray spectroscopy of nuclei with large deformations

Results from GAMMASPHERE

P. Fallon[a]

Lawrence Berkeley National Laboratory, 1 Cyclotron Road, Berkeley, CA 94720, USA

Received: 9 December 2002 /
Published online: 17 February 2004 –

Abstract. The large multidetector gamma-ray arrays (such as GAMMASPHERE, EUROBALL, and GASP) have played a central role in nuclear-structure studies during the past decade. In this paper I will discuss recent results from experiments on nuclei with very large deformations, including: the measurement of the spins, parities, and excitation energies of superdeformed bands in ^{152}Dy; the observation of extreme deformations in ^{108}Cd and the evidence for hyper-intruder states; the study of superdeformed nuclei around $A \sim 40$, which provide an opportunity to test our microscopic understanding of collective excitations; and lifetimes of strongly deformed triaxial bands in ^{163}Lu. I will conclude with a brief discussion on the next generation gamma-ray detector array, GRETA.

PACS. 21.10.Re Collective levels – 23.20.Lv γ transitions and level energies – 21.10.Tg Lifetimes – 29.30.Kv X- and γ-ray spectroscopy

1 Introduction

GAMMASPHERE [1] is the premier gamma-ray detector facility in the US. It consists of up to 110 large-volume coaxial germanium detectors and each germanium detector is surrounded by a bismuth germanate (BGO) anti-Compton shield. This arrangement provides a high total photopeak efficiency (approaching 10% for a 1 MeV gamma-ray) and good peak to background. GAMMASPHERE and EUROBALL [2], the comparable detector array in Europe, are examples of the current state-of-the-art multidetector gamma-ray arrays. Over the past decade the sensitivity of GAMMASPHERE has been greatly enhanced by the addition of a suite of auxiliary detector systems, many of which were designed specifically for GAMMASPHERE.

The large sensitivity of GAMMASPHERE has led to a broad science program ranging from nuclear structure to astrophysics to tests of the standard model. Examples in the areas of fundamental interactions and nuclear astrophysics include: tests of the conserved vector current hypothesis and unitarity of the CKM matrix via a precision measurement of the ^{10}C beta-decay branching ratio [3]; using positronium decays to test QED and C-violation [4]; measuring beta-gamma angular correlations in ^{22}Na to study weak currents [5]; and determining the lifetime of ^{54}Mn [6], which is used as a cosmic chronometer. However, the main focus of the GAMMASPHERE program has been in the area of nuclear structure. These studies have been extremely successful and have extended our understanding of both the structure and fundamental excitations of nuclei and how they change with isopspin, angular momentum, deformation, excitation energy, and mass. Each of these limits isolates a particular facet of nuclear structure and together provide a comprehensive view of the many properties displayed by the nucleus.

It will not be possible to give an overview of the full GAMMASPHERE program and I have chosen to discuss one area, the angular-momentum degree of freedom. I will conclude with a brief discussion on the next generation gamma-ray detector array, GRETA.

2 Rotating nuclei with large deformations

The nucleus is a complex quantal system and its rotational behavior is a powerful probe of nuclear properties. It can be used to alter the underlying nuclear structure (both the macroscopic and microscopic structure) so that new phenomena may emerge (such as superdeformation, shears bands, and the chiral and wobbling modes present in triaxial nuclei), or it can be used to investigate basic nuclear properties, such as pairing excitations or the single-particle structure. The study of "delayed" alignments in ^{72}Kr [7,8] and the recent observation of high spin states in ^{254}No [9,10] fall into this latter category.

In the remainder of this section I will highlight some recent results on the study of very deformed nuclei.

[a] e-mail: pfallon@lbl.gov

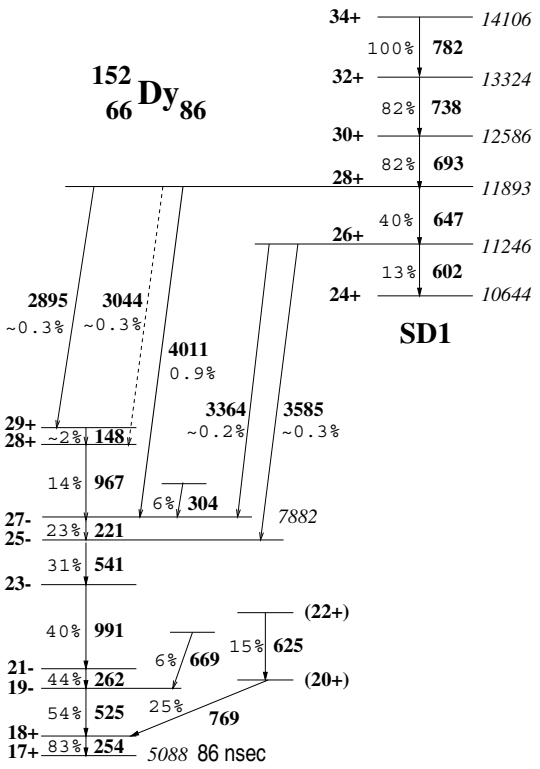

Fig. 1. Partial level scheme of ^{152}Dy showing the gamma-decays from the yrast SD band to the normal deformed states.

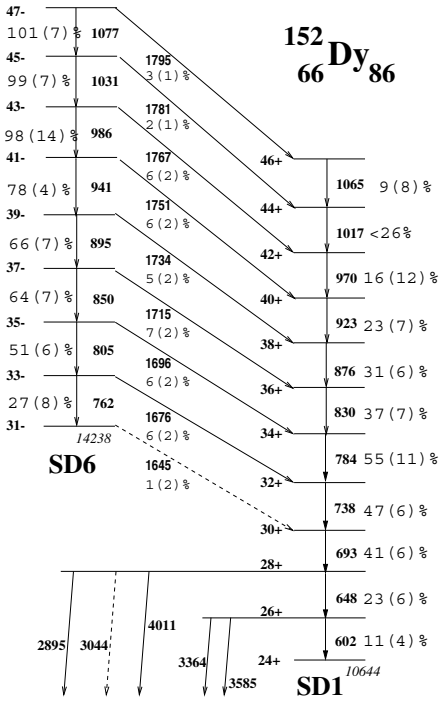

Fig. 2. Partial level scheme showing the gamma-decays from the SD band 6 to the yrast SD band.

2.1 Linking the superdeformed bands in ^{152}Dy

The first superdeformed (SD) band was observed in ^{152}Dy [11] and since then approximately 200 SD bands have been reported in several mass regions ranging from $A \sim 40$ to $A \sim 200$. However, except in a handful of cases (see references in [12]), we have not been able to observe the discrete gamma-rays connecting the SD band to the normal deformed states. As a consequence we do not know such basic nuclear properties as the level spins, excitation energies, and parities for most SD bands. These quantities are needed if we are to fully understand their microscopic structure, the magnitudes of SD shell gaps, and the decay mechanism from the SD minimum to the normal deformed minimum.

In a recent GAMMASPHERE experiment [12] the discrete gamma-ray transitions connecting the yrast SD band in ^{152}Dy to the known normal deformed states were observed. A ^{48}Ca beam at an energy of 191 MeV (mid target) was used to bombard a stack of two 0.4 mg/cm^2 self-supporting ^{108}Pd foils. The experiment used 12 days of beam time and GAMMASPHERE had 100 detectors at the time.

The level scheme showing the discrete gamma-ray decays from the yrast SD band is summarized in fig. 1. The placement of the 4011 keV line as a single-step decay establishes the excitation energy of the SD band. An angular distribution analysis showed that the 4011 keV gamma-ray is consistent with a stretched or un-stretched dipole transition, and from the deduced transition rates this gamma-ray is most likely to be $E1$ rather than $M1$. Thus, the band is assigned positive parity (in agreement with theoretical expectations) and the lowest SD state has a spin of either 22 or 24 $\hbar$. Furthermore, the 4011 keV gamma-ray was found to have a partial lifetime of ~ 2.9 ps, which translates to a $B(E1)$ of $\sim 2 \times 10^{-6}$ W.u. This retarded $B(E1)$ value is similar to that reported in the decay of $A \sim 190$ SD bands and is a measure of the coupling of SD and normal deformed states.

Having firmly established the 4011 keV transition as a one-step decay, the remaining gamma-rays could be placed and these fix the level spins of the SD band as shown in fig. 1.

The properties of excited SD bands provide information on the basic excitation modes within the superdeformed minimum, and by observing the decays between SD bands it is possible to gain insight into the nature of these excitations. While one may expect that the low-density of states associated with the SD shell gap could allow low-lying collective modes to compete with single-particle excitations, the experimental data indicates the dominance of single-particle excitations. Nevertheless, in the $A \sim 190$ region there are a few cases (see references in [13]) where the observed interband decays provide compelling evidence for collective octupole vibrations in a superdeformed nucleus. There was also evidence for octupole collectivity in superdeformed ^{152}Dy, where it was reported [14] that one of the excited bands (band 6) decayed to the yrast SD band (band 1); however, no interband linking decays were observed in this data set.

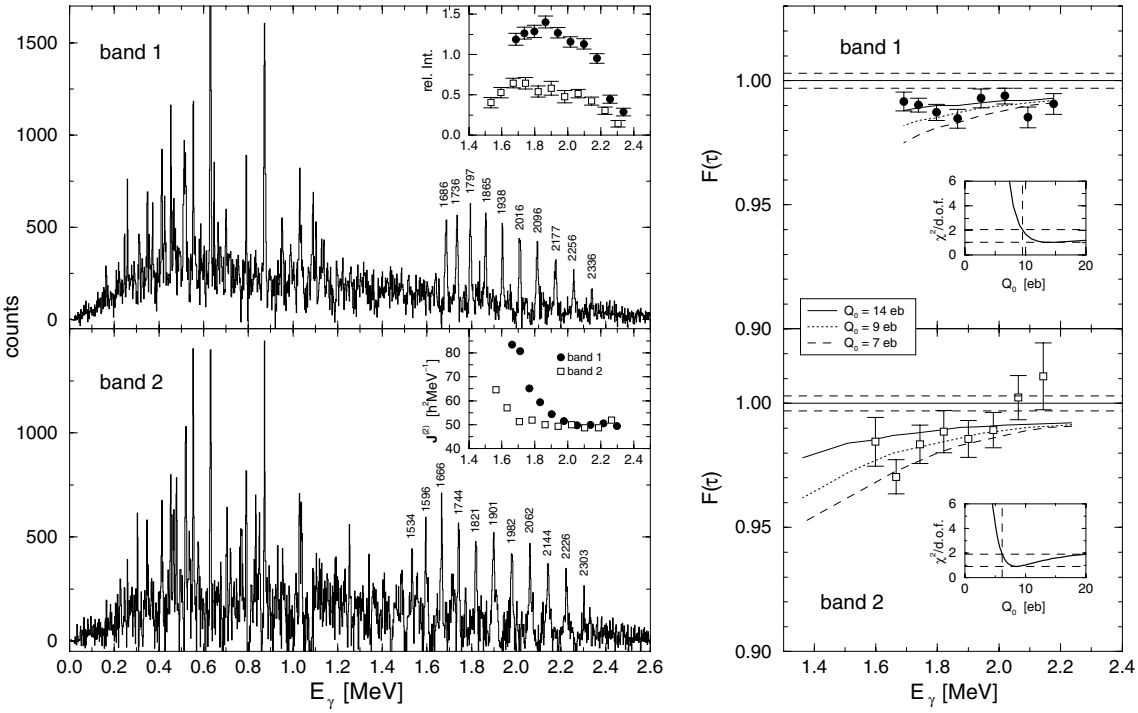

Fig. 3. Left: spectra of bands 1 and 2 in ^{108}Cd. The insets show the relative intensities of the bands with respect to the total intensity of the reaction channel (upper panel), and the dynamic moments of inertia (lower panel). The values for band 1 are given by the full circles, those for band 2 by the open squares. Right: results of the fractional Doppler shift analysis. The lines show examples for calculated $F(\tau)$ curves. The χ^2 fits for the calculated curves to the data as a function of the quadrupole moment Q_0 are shown in the insets. The horizontal dashed lines represent the minimal value $\chi^2_{\rm min}$ and $\chi^2_{\rm min}+1$. The vertical dashed lines indicate the lower limit of the quadrupole moment consistent with a 1σ error.

In the present high-statistics GAMMASPHERE experiment the decay of band 6 to band 1 was confirmed and nine interband transitions were identified [13] (fig. 2). These newly observed gamma-rays give the absolute excitation energy of band 6 and its excitation energy (~ 1.3 MeV) relative to band 1. Furthermore, the angular distributions of the interband transitions are consistent with them being dipole transitions (the $J \rightarrow J-1$ solution is favored by the authors), and an estimate of their partial half-lives favors $E1$ character. Band 6 is thus assigned negative parity and odd spins. The measured properties of these decays are found to be consistent with band 6 being a collective octupole vibration in agreement with RPA calculations [15], which predict collective octupole states in superdeformed ^{152}Dy.

2.2 Very extended shapes in ^{108}Cd

It is possible that some nuclei may attain even greater quadrupole deformations than those observed in superdeformed nuclei and the search for such hyperdeformed (HD) shapes has been a goal of nuclear structure for many years. As an extreme limit, hyperdeformed nuclei have a deformation corresponding to a prolate axis ratio of $c/a = 3$. In this same limit, based on a simple harmonic-oscillator potential, superdeformed nuclei have $c/a = 2$, and both HD and SD shapes are favored due to the special symmetries associated with integer axis ratios, which lead to large shell gaps that help to stabilize the nuclear deformation. However, realistic nuclear potentials modify this simple picture and superdeformed nuclei have axis ratios in the range $c/a \sim 1.6$ to 1.8. Similarly, we may expect hyperdeformed nuclei to exhibit c/a values smaller than 3. A classification of the shape (*e.g.*, normal deformed, superdeformed, or hyperdeformed) that does not depend on the absolute value of c/a is therefore advantageous and I will return to this question later.

An experiment to search for the predicted [16] very extended nuclear shapes ($c/a \sim 2.3$) in ^{108}Cd was performed on GAMMASPHERE using the reaction ^{48}Ca(^{64}Ni,4n) at 207 MeV. Two rotational bands were observed [17,18] at very high angular momentum and these are shown in fig. 3. The bands carry about 1.4% and 0.6% of the intensity of the ^{108}Cd channel. No decays were seen linking the bands to the known normal deformed states; however, it is estimated (assuming $\Im^{(1)} = \Im^{(2)}$) that they extend over a spin range from about 40 to 60 $\hbar$. The bands have large dynamic moments of inertia ($\Im^{(2)}$), shown in the inserts to fig. 3, consistent with a very large prolate deformation of $c/a \sim 1.8$. A measure of the transition state lifetimes (via the slowing-down of the recoil in the target) confirmed their large deformation. Band 1 has a lower limit for the quadrupole moment of $Q_0 = 9.5$ eb. The transitions were too fast to set a reliable upper limit. Band 2 has a $Q_0 = 8.5$ eb with a lower limit of 6.2 eb and once more it was not possible to set a meaningful upper limit.

These two new bands are clearly very deformed (at least superdeformed), but what is their structure? An answer to this was found in their dynamic moments of inertia. Both bands exhibit a rapid increase in $\Im^{(2)}$ at the lowest frequencies, which is often a sign of a change in the microscopic configuration. Recent calculations [19] suggest that there is indeed a change in configuration in band 1 and that the rise in $\Im^{(2)}$ coincides with the occupation of the proton $i_{13/2}$ intruder state.

The proton $i_{13/2}$ intruder is a very exotic orbital to be occupied at such a low atomic number, $Z = 48$. It starts out at the Fermi surface for spherical nuclei around $Z = 100$ and for normal deformed ($\beta_2 \approx 0.2$) nuclei around $Z = 92$. In this region the $i_{13/2}$ proton is the *normal-intruder* state, which is lowered by one oscillator shell due to the spin-orbit interaction. Intruder states have large quadrupole moments and they are lowered even further by increasing the quadrupole deformation until at superdeformations ($\beta_2 \approx 0.6$) the $i_{13/2}$ state is at the Fermi surface for $Z \approx 66$ (*e.g.*, ^{152}Dy). At this point, the $i_{13/2}$ intruder has dropped two major oscillator shells ($N - 2$) and it can be classified as a *super-intruder*[1]. By the time we get to cadmium, $Z = 48$, the $i_{13/2}$ state has come down 3 major shells, and it seems natural to label this orbital a *hyper-intruder* ($N - 3$).

These new bands in ^{108}Cd provide evidence for the occupation of a *hyper-intruder* and suggest the exciting possibility that hyperdeformed nuclei could be observed. Of course, the next step would be to identify the neutron *hyper-intruder*, which is the $j_{15/2}$ state in the cadmium $N \approx 60$ region. Calculations [20] suggest we are tantalizingly close and that the $j_{15/2}$ intruder approaches the Fermi surface at $N = 64$, *i.e.* ^{112}Cd.

2.3 Highly deformed bands in A $\sim$ 40 nuclei

Recent GAMMASPHERE experiments, using the charged-particle detector Microball [21], have revealed the existence of highly deformed rotational structures in several A$\sim$ 40 nuclei, including ^{36}Ar [22] and ^{40}Ca [23]. The first example used the reaction ^{24}Mg(^{20}Ne,2α)^{36}Ar at a beam energy of 80 MeV, the second used the reaction ^{28}Si(^{20}Ne,2α)^{40}Ca at 84 MeV. In both cases it was possible to link the observed bands to the known level scheme (thus determining their spins, parities, and excitation energies) and to measure the state lifetimes and thus extract $B(E2)$ values. The $B(E2)$ values are consistent with highly collective structures with large deformations of the order of $\beta_2 \sim 0.5$.

The ^{36}Ar and ^{40}Ca deformed structures are interpreted as core excitations from the *sd* to the *pf* shell. In particular the $f_{7/2}$ $N = 3$ intruder is occupied (fig. 4): ^{36}Ar has 2 protons and 2 neutrons in the Nilsson [330]1/2 state, while ^{40}Ca has 2 protons and 2 neutrons in the Nilsson [330]1/2 state and a further 2 protons and 2 neutrons in the [321]3/2 state, making it an 8p-8h excitation. It is interesting to note that the lowest few states of the proposed 8p-8h band in ^{40}Ca were known previously, but it was not until one had established the full rotational band that the assignment as an 8p-8h band could be made with confidence.

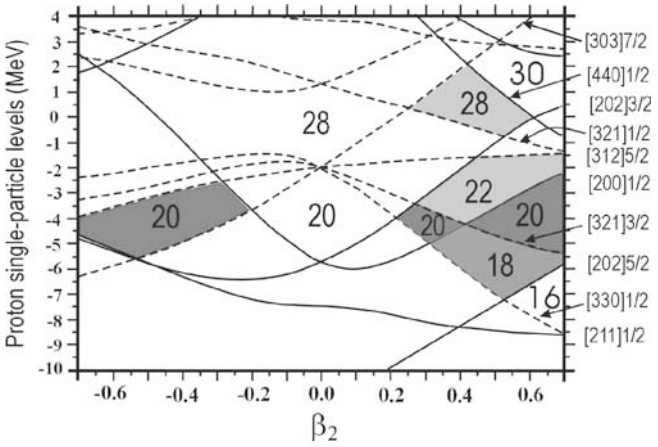

Fig. 4. Woods-Saxon single-particle energy levels as a function of deformation. Solid (dashed) lines are used for positive (negative) parity. Large spherical and deformed shell gaps are indicated by their particle numbers.

A major goal of these studies has been to further understand the microscopic structure of rotational collective excitations, that is, to make the connection between the deformed intrinsic states and the microscopic wave functions. However, for all but the very lightest nuclei truncations and approximations to the theory are necessary and these must be tested by experiment. It turns out that the region around $A \sim 40$ nuclei is an ideal place to do this. It is a region where deformed shell gaps are characterized by intruder states ($f_{7/2}$) originating from the next higher oscillator shell, but the limited valence space is still sufficiently small to make large-scale shell model calculations tractable.

With the essentially complete spectroscopic information now available for $A \sim 40$ deformed bands these data are proving to be a critical benchmark for a wide range of theoretical models, including large-scale shell models, the projected shell model, cranked Nilsson-Strutinsky, relativistic mean field, Hartree-Fock, and generator coordinate methods (see refs. [22] and [24] for details).

2.4 Lifetimes of the wobbling band in ^{163}Lu

The wobbling phonon was predicted over 30 years ago as a unique mode of excitation that can occur in a nucleus which has a stable triaxial deformation. It corresponds to the situation where the collective angular momentum R moves away from a principal axis. The rotational frequency precesses around R and the motion can be characterized as a collective (wobbling) phonon. The different rotational bands are labeled by the number of wobbling phonons, n_w. Recently, the first evidence for the existence of the wobbling mode was seen in ^{163}Lu [25]. The reader

[1] In general, the occurrence of superdeformed nuclei can be correlated with the occupation of intruder states not from one but from but two major oscillator shells above, and in analogy we may expect hyperdeformed nuclei to involve intruder orbitals from three shells above.

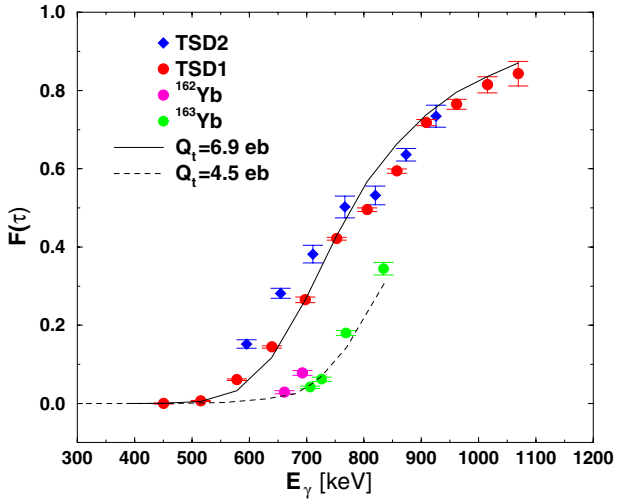

Fig. 5. Fraction Doppler shift curves for triaxial and normal deformed bands in ^{163}Lu. The solid and dashed lines are calculated $F(\tau)$ curves.

is referred to ref. [26] for a more detailed discussion of triaxial bands in the $A \sim 170$ region.

Here, I simply wish to show one very new result on the lifetimes of the wobbling phonon band in ^{163}Lu. In a GAMMASPHERE experiment using the reaction ^{44}Ca + ^{123}Sb (gold-backed target) at 190 MeV, the lifetimes of the lowest-lying triaxial strongly deformed band (TSD1) and the first-excited triaxial band (TSD2) were determined using the Doppler shift attenuation method. TSD2 is the proposed single-wobbling-phonon excitation ($n_{\rm w} = 1$) built on band 1 ($n_{\rm w} = 0$).

The preliminary results of this experiment are shown in fig. 5, which contains the measured fractional Doppler shifts ($F(\tau)$) for TSD1, TSD2, and a number of normal deformed prolate states included for comparison. The TSD bands and the normal deformed bands are clearly separated. The latter were found to have a $Q_{\rm t} = 4.5$ eb consistent with previous measurements. The triaxial bands have a significantly larger quadrupole moment ($Q_{\rm t} = 6.9$ eb) consistent with a larger deformation. For our purposes, however, the absolute value of $Q_{\rm t}$ is not so important as the fact that TSD1 and TSD2 have identical quadrupole moments suggesting identical deformations, which is what one would expect if the bands are indeed the $n_{\rm w} = 0$ and $n_{\rm w} = 1$ members of a wobbling phonon multiplet. Moreover, these data will also provide a direct measure of the transition strengths of the interband TSD2 to TSD1 decays, which is complementary to previous measurements and an important indicator of the collectivity of the excitation mode.

3 GRETA, Gamma-Ray Energy Tracking Array

Gamma-ray detection has played an important role in nuclear physics. New scientific insights have come with each improvement in the detector technology. I will discuss a next generation gamma-ray detector (the Gamma-Ray Energy Tracking Array, GRETA [27]), which is based on a close-packed geometry and will comprise about 100 highly segmented coaxial HPGe detectors. (See ref. [28] for a discussion on the comparable European project, AGATA.) GRETA and AGATA will use the new concept of gamma-ray energy tracking to give the position and energy deposition of every gamma-ray interaction in the detector. These new detectors promise another factor of 100 to 1000 gain in sensitivity compared to current arrays for a broad range of nuclear-physics studies. Gamma-ray energy tracking was first proposed by LBNL in 1994. It takes advantage of the recent advances in detector segmentation, digital electronics, and computing power.

Present arrays use BGO shields to suppress Compton events; this means that about 50% of the 4π coverage is essentially "wasted" and it has long been realized that the optimal 4π device would use only Ge. For a 4π Ge shell to work, and still be feasible, one needs to use highly segmented detectors. The idea is to have enough segmentation to follow (track) the individual interaction points of an incident gamma-ray so that one can reconstruct its full energy without summing the interactions from different gamma-rays. Thus the challenge has been to: 1) produce highly segmented crystals with good signal-to-noise characterics; 2) develop algorithms to extract the 3-dimensional positions of each gamma-ray interaction; 3) develop algorithms to reconstruct the full energy of the gamma-ray from these individual interactions (this is done via tracking, which takes advantage of the angle energy relationship in the Compton scatter formula).

To reconstruct the energies of multiple gamma-rays one needs to locate the position of the interactions to within a few mm. This could be done, in principle, by having segments that are of the order of few mm themselves, but this would require about a hundred segments per crystal, which is simply not feasible. A key breakthrough for coaxial detectors was the realization that one can use segments that are about 1-2 cm and still recover the desired few mm position resolution. This is done by using the signals induced in the neighboring segments (*i.e.* those adjacent to the one that collects the full charge) to *interpolate* to where the interaction occurred.

A great deal of R&D has been done over the past 8 years, which has demonstrated proof-of-principle in the three main areas of gamma-ray tracking R&D: segmented detector technology; signal analysis and decomposition; and event tracking. Measurements were carried out primarily using the 36-segment GRETA prototype detector at LBNL. The detector was found to have good energy resolution (about 1.9 keV for 1.33 MeV, and 1.2 keV for 60 keV gamma-rays) and the position of a single interaction within a segment could be determined with an accuracy of about 1-2 mm in all 3 dimensions [29]. Recently, a comprehensive comparison of the simulated and measured signals from a ^{137}Cs source was carried out [30]. In these measurements most of the segments were instrumented with digital electronics and the full analysis procedure of signal decomposition and tracking was applied to the data. The simulated data were treated with exactly the same

Table 1. Resolving power (RP) of GRETA for different experimental conditions and assuming a solid-angle coverage of 80% and a position resolution of 2 mm.

Reaction	E (MeV)	v/c	γ-ray Multiplicity	GRETA RP (absolute)	RP (Rel. to GAMMASPHERE)
Stopped nuclei	5.0	0.0	4	2.1×10^7	200
High-spin normal kinematics	1.0	0.04	20	2.4×10^6	55
High-spin inverse kinematics	1.0	0.07	20	2.2×10^6	120
Coulex/transfer	1.5	0.1	15	3.7×10^6	510
Fragmentation in-beam	1.5	0.5	6	5.9×10^6	12500
Fragmentation Coulex	5.0	0.5	2	2.7×10^3	110

analysis procedure as the measurement. An algorithm based on the least-square method was used for the signal analysis, which can handle up to 4 segments each with 2 interactions. The efficiency of this method of locating a single interaction in one segment to within 1 mm is 85%. The measurement and simulation agree with each other for both the raw spectra and the spectra after tracking. As expected for a single crystal, the tracking improves the peak-to-total ratio from $\sim 16\%$ to $\sim 30\%$, but does not increase the efficiency. These results indicate that we have an accurate understanding of the signals from the prototype and all the necessary data analysis algorithms are functioning.

Future research and development plans include: additional measurements with the prototype; obtaining a three-crystal detector module; improving both the signal analysis and tracking algorithms; developing digital electronics. Our next step in detector prototyping is a three-crystal detector module. The crystals will be 9 cm long with a tapered regular hexagon shape and have 36 segments, like the previous prototype, but the diameter of the crystals before they are shaped will be 8 cm rather than 7 cm. The three crystals will be close-packed in one cryostat with a gap of less than 3.5 mm between the crystals and 4.5 mm between the crystals and the cryostat walls. We expect to receive this prototype in one year.

An electronics module for signal digitizing is being developed. The first version will have eight input channels and provide energy, time, and pulse shape information. Each channel can generate and accept an independent trigger, and the data are read out via a VME bus. The ADCs have a sampling rate of 100 MHz and a resolution of 12 bits. This module is being tested and the initial indication is that it is performing to specifications. Based on the experience gained from this module, we will design a 40-channel board capable of processing all the signals and providing the positions and energies of all interactions in one crystal. Currently, we envision that the construction of GRETA can be completed in eight years and, prior to this, experiments will be carried out during an "early implementation" phase.

A 4π tracking array, such as GRETA, promises tremendous gains in experimental sensitivity and new scientific opportunities. As shown in table 1, GRETA will have a resolving power that is 100 to 1000 (or more) times higher than GAMMASPHERE, depending on the type of experiment. This will serve to extend the cross-section limits of typical in-beam gamma-ray studies from micro-barns to nano-barns and push the frontiers of nuclear physics to higher angular momentum, higher excitation energy, further from the line of stability, and to heavier elements.

I would like to thank Torben Lauritsen, Carl Svensson, and Chris Chiara for providing materials presented in this paper, and all members of the nuclear-structure group at Berkeley for fruitful discussions and comments. This work has been supported in part by the U.S. DoE under contract No. DE–AC03–76SF00098.

References

1. I-Y. Lee, Nucl. Phys. A **520**, 641c (1990).
2. W. Korten, this issue, p. 5.
3. B.K. Fujikawa *et al.*, Phys. Lett. B **449**, 313 (1999).
4. P.A. Vetter, S.J. Freedman, Phys. Rev. A **66**, 052505 (2002).
5. C.J. Bowers *et al.*, Phys. Rev. C **59**, 1113 (1999).
6. K. Zaerpoor *et al.*, Phys. Rev. Lett. **79**, 4306 (1997).
7. S. Fischer *et al.*, Phys. Rev. Lett. **87**, 132501 (2001).
8. N.S. Kelsall *et al.*, this issue, p. 131.
9. P. Reiter *et al.*, Phys. Rev. Lett. **82**, 509 (1999).
10. P.T. Greenlees, this issue, p. 87.
11. P.J. Twin *et al.*, Phys. Rev. Lett. **57**, 811 (1986).
12. T. Lauritsen *et al.*, Phys. Rev. Lett. **88**, 042501 (2002).
13. T. Lauritsen *et al.*, to be published in Phys. Rev. Lett.
14. P.J. Dagnall *et al.*, Phys. Lett. B **335**, 313 (1994).
15. T. Nakatsukasa, K. Matsuyanagi, S. Mizutori, W. Nazarewicz, Phys. Lett. B **343**, 19 (1995).
16. R.R. Chasman, Phys. Rev. C. **64**, 024311 (2001).
17. R.M. Clark *et al.*, Phys. Rev. Lett. **87**, 202502 (2001).
18. A. Goergen *et al.*, Phys. Rev. C. **65**, 027302 (2001).
19. C.T. Lee *et al.*, Phys. Rev. C. **66**, 041301(R) (2002).
20. Y. Sun, private communication.
21. M. Devlin *et al.*, Nucl. Instrum. Methods Phys. Res. A **383**, 506 (1996).
22. C.E. Svensson *et al.*, Phys. Rev. Lett. **85**, 2693 (2000).
23. E. Ideguchi *et al.*, Phys. Rev. Lett. **87**, 222501 (2001).
24. A. Poves *et al.*, this issue, p. 119.
25. S. Odegard *et al.*, Phys. Rev. Lett. **86**, 5866 (2001).
26. G.B. Hagemann, this issue, p. 183.
27. M.A. Deleplanque *et al.*, Nucl. Instrum. Methods Phys. Res. A **430**, 292 (1999).
28. J. Gerl, *Future nuclear spectroscopy with RISING and AGATA*, talk given at the NS2002 conference.
29. K. Vetter *et al.*, Nucl. Instrum. Methods Phys. Res. A **452**, 105 (2000); **223**, 223 (2000).
30. A. Kuhn, PhD Thesis, UC Berkeley (2002), LBNL-51726.